

Published in final edited form as:

*Stem Cell Res.* 2011 July ; 7(1): 75–88. doi:10.1016/j.scr.2011.04.002.

## Loss of the chromatin regulator MRG15 limits neural stem/progenitor cell proliferation via increased expression of the p21 Cdk inhibitor

Meizhen Chen<sup>a</sup>, Olivia M. Pereira-Smith<sup>a,b</sup>, and Kaoru Tominaga<sup>a,b,\*</sup>

<sup>a</sup> Barshop Institute for Longevity and Aging Studies, University of Texas Health Science Center at San Antonio, San Antonio, Texas 78245, USA

<sup>b</sup> Department of Cellular and Structural Biology, University of Texas Health Science Center at San Antonio, San Antonio, Texas 78245, USA

### Abstract

Chromatin regulation is crucial for many biological processes such as transcriptional regulation, DNA replication, and DNA damage repair. We have found it is also important for neural stem/progenitor cell (NSC) function and neurogenesis. Here, we demonstrate that expression of the cyclin-dependent kinase inhibitor p21 is specifically up-regulated in *Mrg15* deficient NSCs. Knockdown of p21 expression by p21 shRNA results in restoration of cell proliferation. This indicates that p21 is directly involved in the growth defects observed in *Mrg15* deficient NSCs. Activated p53 accumulates in *Mrg15* deficient NSCs and this most likely accounts for the up-regulation of p21 expression in the cells. We observed decreased p53 and p21 levels and a concomitant increase in the percentage of BrdU positive cells in *Mrg15* null cultures following expression of p53 shRNA. DNA damage foci, as indicated by immunostaining for  $\gamma$ H2AX and 53BP1, are detectable in a sub-population of *Mrg15* deficient NSC cultures under normal growing conditions and the majority of p21-positive cells are also positive for 53BP1 foci. Furthermore, *Mrg15* deficient NSCs exhibit severe defects in DNA damage response following ionizing radiation. Our observations highlight the importance of chromatin regulation and DNA damage response in NSC function and maintenance.

### Keywords

. Neural precursor cell; cell proliferation; chromatin; epigenetics; gene expression; DNA damage response

---

Establishment and maintenance of a functional central nervous system depends on multipotent and self-renewable neural stem/progenitor cells (NSCs) during development and also in adult brain [1, 2]. The self-renewal ability of NSCs is essential for maintaining the stem cell pool for brain development and replacement of cells in the brain during the life span of an organism [3, 4]. NSCs also supply three major differentiated cell types: neurons,

---

© 2011 Elsevier B.V. All rights reserved.

\*Correspondence: Kaoru Tominaga, Ph.D., Barshop Institute for Longevity and Aging Studies, Department of Cellular and Structural Biology, University of Texas Health Science Center at San Antonio, 15535 Lambda Drive, STCBM #3.100, San Antonio, TX 78245, USA. Tel.: +1-210-562-5067; Fax: +1-210-562-5093; tominaga@uthscsa.edu.

**Publisher's Disclaimer:** This is a PDF file of an unedited manuscript that has been accepted for publication. As a service to our customers we are providing this early version of the manuscript. The manuscript will undergo copyediting, typesetting, and review of the resulting proof before it is published in its final citable form. Please note that during the production process errors may be discovered which could affect the content, and all legal disclaimers that apply to the journal pertain.

astrocytes, and oligodendrocytes in the brain for differentiation into restricted progenitor cells [5, 6]. Therefore, maintaining the appropriate balance between self-renewal and multilineage differentiation in NSCs is critical for development of functional brain networks in adults as well as during embryonic development.

Chromatin structure can be dynamically changed by covalent modifications of histone tails such as acetylation and methylation. Chromatin regulation via these modifications is involved in many important biological processes such as transcription, DNA replication and DNA damage repair. Chromatin regulation is also important for NSC function and neurogenesis [7–12]. The brain-specific knockout of Mll1 (mixed-lineage leukemia 1), a histone H3 lysine 4 (H3K4) methyltransferase in mice, exhibits severely impaired neurogenesis [13]. Chromatin at the *Dlx2* gene, which is a key downstream regulator of neurogenesis, is bivalently marked by both H3K4me3 and H3K27me3 and the *Dlx2* gene fails to activate in Mll1-deficient NSCs. Haploinsufficiency or knockdown of CBP (CREB binding protein) the histone acetyltransferase inhibits differentiation of embryonic NSCs into all three lineages and this most likely explains the cause of cognitive dysfunction in Rubinstein-Taybi syndrome where one allele of CBP is deleted or mutated [14]. Interestingly, it has been recently shown that deregulation of histone H4 lysine 12 (H4K12) acetylation is associated with age-dependent memory impairment in the hippocampus in which NSCs are located [15]. This correlates with the loss of initiation of a hippocampal gene expression program associated with memory consolidation in aged mice. HDAC2 but not HDAC1 negatively regulates memory formation and memory-related gene expression through modulation of histone acetylations such as H4K5 and H4K12 in the hippocampus [16]. Therefore, epigenetic mechanisms play crucial roles in NSC function and neurogenesis by modulating important changes in gene expression.

MRG15 was initially isolated as a member of gene family that is related to cellular senescence and cell growth control and is evolutionarily highly conserved [17–19]. MRG15 has a chromodomain in the N-terminus [20–22] and can directly bind to di- or tri-methylated histone H3 at lysine 36 (H3K36me) through this domain [23–25]. It has been shown that MRG15 forms complexes with both histone acetyltransferases (HATs) and histone deacetylases (HDACs) [26–37]. Although a role of MRG15-containing mSin3/HDAC complex in mammals still remains unknown, similar complex in budding yeast, named Rpd3S, is important for deacetylation of coding regions to suppress spurious intragenic transcription through H3K36me recognition [38, 39]. Defect of a homologous complex in fission yeast causes increased accessibility of DNA to genotoxic agents and widespread antisense transcripts that are processed at coding regions and abrogates global protective functions of chromatin [40]. MRG15 is also a stable component of Tip60 HAT complex, which is implicated in transcriptional control as well as DNA repair and apoptosis [41]. Purification of the *Drosophila* Tip60 complex demonstrated that the components of the fly complex were very similar to those in the mammalian complex [42]. Moreover, it is evident that Tip60 and MRG15 are essential components of this complex, as knockdown or deletion of either gene results in an inability to repair DNA double strand breaks (DSBs) as well as embryonic lethality. We, and others, have shown that MRG15 and Tip60 are both important for DNA DSB repair [43–45].

We have previously published that embryonic *Mrg15* null NSCs exhibit defects in growth as well as neuronal lineage differentiation [46]. In this study, we have examined the molecular mechanism(s) of the growth defect underlying *Mrg15* deficiency in mouse embryonic NSCs by comparing neurosphere cultures obtained from *Mrg15* null and wild-type embryonic brains. We have found increased expression of p21<sup>Sdi1/Cip1/Waf1</sup> (p21) in *Mrg15* null NSC cultures that most likely leads to the growth defect observed in *Mrg15* deficient cells,

and provide evidence that inefficient DNA damage repair in *Mrg15* null NSCs may contribute to this growth defect.

## EXPERIMENTAL PROCEDURES

### Animals

*Mrg15* heterozygous mice were maintained under pathogen-free conditions with approval of the institutional animal care committee and were treated in accordance with the NIH Guide for the Care and Use of Laboratory Animals. We used a mixed genetic background (C57BL/6J and 129SvEv) of mice in this study [47] as backcrossing to the C57BL/6 background exacerbated the fetal phenotype.

### Neural Stem/Progenitor Cell (NSC) Culture

Cerebral cortices of timed pregnant mouse embryos (E10.5) were dissociated, single cells obtained by trypsin digestion following trituration with a polished pasteur pipette and cultured in 35-mm tissue culture dishes (Corning Incorporated, Corning, NY, USA) in Neurobasal Medium (Gibco-BRL, Gaithersburg, MD, USA) supplemented with 20 ng/ml FGF-2/basic FGF (Upstate, Temecula, CA, USA), 20 ng/ml EGF (BD Bioscience, Bedford, MA, USA), 2 mM L-glutamine, 1 x B27, and 50 U/ml penicillin-50 mg/ml streptomycin (Gibco-BRL, Gaithersburg, MD, USA). The cells were maintained in a humidified incubator at 37°C in 95% air/5% CO<sub>2</sub> for one week and neurospheres were isolated. Isolated neurospheres were trypsinized, cells were counted using a hemocytometer and used for the next experiments.

### PCR array and quantitative RT-PCR (qRT-PCR)

Total RNA was isolated from neurospheres lysed with Trizol Reagent (Invitrogen) and purified with the RT<sup>2</sup> qPCR-Grade RNA Isolation Kit (SABiosciences, PA-001). Elimination of contaminating DNA and cDNA synthesis was performed with RT<sup>2</sup> First Strand Kit (SABiosciences, C-03) and real-time PCR performed by ABI Prism 7500 sequence detector (Applied Biosystems) using the RT2 Profiler<sup>TM</sup> PCR Array Mouse Cell Cycle (SABiosciences, PAMM-020A), according to manufacturer's instructions. Data analyses were performed using the PCR Array Data Analysis Web Portal.

For qRT-PCR, cDNAs were synthesized from neurosphere derived total RNA (0.3 µg) by priming with 200 ng of random hexamer, 0.5 mM dNTP and 100 units of SuperScript II Reverse Transcriptase (Invitrogen) at 42°C for 1 h. Real-time PCR was carried out using SYBR® Green PCR Master Mix (Invitrogen). Fluorescence was monitored by GeneAmp 7900HT Sequence Detection system. Expression levels of target genes were normalized to those of β-actin. The following primer sets were used; p21-5' (5'-GCAGATCCACAGCGATATCCAG-3') and p21-3' (5'-CGAAGAGACAACGGCACACTTT-3'), p16-5' (5'-CGAACTCTTTCGGTCGTACCC-3') and p16-3' (5'-CGAATCTGCACCGTAGTTGAGC-3'), p19-5' (5'-GTTCTTGGTCACTGTGAGGATTCAG-3') and p19-3' (5'-CCATCATCATCACCTGGTCCAG-3'), β-actin-5' (5'-ACCAGTTCGCCATGGATGAC-3') and β-actin-3' (5'-TGCCGGAGGCGTTGTC-3'). The unpaired t test was used for statistical analyses.

### Western blots

The cells were washed with PBS and lysed with lysis buffer (20 mM Tris-HCl [pH 7.5], 1% NP-40, 150 mM NaCl, 10% glycerol, and protease inhibitor cocktail set I [Calbiochem]). The lysates were kept on ice for 30 min and centrifuged at 20,000×g for 15 min. Protein concentration of the supernatants was determined by the Bradford protein assay (Bio-Rad)

using BSA as a standard. The total proteins were separated on 12.5% or 8% SDS-PAGE and transferred to nitrocellulose membrane. Membranes were blocked in 2% goat serum/0.5% skimmed milk in PBST (0.05% Tween 20) for 1 h and then probed with primary antibody overnight at 4°C. Primary antibodies used were as follows: rabbit anti-p21 (Santa Cruz, H-164, 1:1000), mouse anti-p21 (BD Biosciences, SXM30, 1:400), rabbit anti-phospho-p53 at Ser15 (Cell Signaling, 9284, 1:1000), rabbit anti-p53 (Vector Laboratories, CM5, 1:1000), rabbit anti-MRG15 (1:1000) [47], and mouse anti-β-actin (abcam, AC-15, 1:5000). Beta-actin was used as a loading control. Horseradish peroxidase-conjugated secondary antibodies (Santa Cruz) were used at 1:4000 for 1 h at room temperature and SuperSignal West system was used for signal detection.

### Lentivirus production

A shRNA construct for p21 and empty vector were obtained from Drs. Phoenix and Temple [48, 49]. This shRNA-expressing lentiviral plasmid was cotransfected with plasmids pMD2.G and psPAX2 into 293T cells. Virus-containing medium was collected at 48 h and 72 h after transfection, filtered, and concentrated by ultracentrifugation. For viral transduction into NSCs, lentivirus-containing medium was added to NSC cultures at a multiplicity of infection (moi) of 10. Virus-containing medium was removed from cultures 24 h after infection and cells were further incubated for 48 h to ensure GFP expression. The GFP-positive infected cells were sorted by FACS, counted, and seeded onto poly-L-lysine-coated coverslips. Two days later, the cells were pulsed with 10 μM BrdU for 1 h and positive cells detected using the immunocytochemistry method using mouse anti-BrdU (BD Biosciences, B44, 1:5) and Alexa Fluor 594-conjugated secondary antibodies (Invitrogen, 1:1000 dilution) described previously [46]. The percentage of BrdU-positive cells was determined by counting under a fluorescent microscope, and at least 200 cells per sample were scored.

A similar approach was used with a lentivirus expressing p53 shRNA (pSicoR p53) [50] and empty vector (pGIPZ), obtained from Dr. Iwakuma.

### Cell cycle analysis

The GFP-positive cells ( $1 \times 10^6$ ) were fixed in 70% ethanol and washed with PBS. The cells were incubated in PBS containing 0.1 mg/ml RNase (Sigma) at 37°C for 30 min and 50 μg/ml propidium iodide (Sigma) was added to each sample. Cells were examined using a FACScalibur (Becton Dickinson) and data were analyzed using CellQuest and ModFit LT softwares.

### Immunofluorescence staining

Cells were plated on poly-L-lysine-coated coverslips and cultured for 2 days with Neurobasal Medium supplemented with B27 and cell growth factors. For γ-irradiation experiments, the cells were exposed to ionizing radiation (IR) at 10 Gy from a <sup>137</sup>Cs source and then incubated until indicated time points. The cells were fixed with 4% paraformaldehyde in PBS for 10 min at room temperature. Fixed cells were washed with PBS and permeabilized with PBST (0.1% Triton X-100) for 10 min at room temperature. Nonspecific binding was blocked with 10% goat serum in PBST for 30 min at room temperature. Cells were incubated with primary antibodies overnight at 4°C. Primary antibodies used were as follows: mouse anti-p21 (BD Biosciences, SXM30, 1:250), mouse anti-γH2AX at Ser139 (Millipore, JBW301, 1:400), rabbit anti-53BP1 (Bethyl, BL182, 1:400), and rabbit anti-RAD51 (Santa Cruz, H-92, 1:200). Cells were washed three times with PBST, then incubated with Alexa Fluor 488 or 594-conjugated secondary antibodies (Invitrogen, 1:1000 dilution) for 1 h at 37°C. After washing the cells were counterstained with 0.1 μg/ml DAPI (4', 6-Diamidino-2-phenylindole, Sigma). Coverslips were mounted

onto Superfrost<sup>®</sup> Microscope Slides (Fisher Scientific) with Fluoro-Gel (Electron Microscope Science) and fluorescent images were acquired using a Zeiss Axiovert 200M microscope with X-Cite<sup>™</sup> 120 fluorescence illumination unit and AxioCam MRm digital camera (Carl Zeiss Inc., Germany). All photographs were taken using X100 oil immersion objective.

## RESULTS

### p21 expression is upregulated in *Mrg15* deficient NSCs

We have previously reported that *Mrg15* deficient NSCs from embryos show severe growth defects in vitro and in vivo [46]. Because BrdU incorporation of *Mrg15* deficient NSCs in culture was significantly reduced compared with those from wild-type, we speculated cell cycle control is dysregulated in *Mrg15* deficient NSCs. To further elucidate the molecular mechanism for this dysregulation in *Mrg15* deficient cells, we used a Mouse Cell Cycle PCR Array and identified p21, a cyclin-dependent kinase inhibitor, as a gene that was upregulated 3.3-fold in *Mrg15* deficient NSCs compared with wild-type cells. We further confirmed that p21 was upregulated at early passage in the majority (80–90%) of cells within 3 independent isolated clones of *Mrg15* deficient NSCs by quantitative RT-PCR (qRT-PCR) (Fig. 1A). We performed statistical analysis using the unpaired t test to determine if the difference in p21 expression levels in wild-type versus *Mrg15* deficient NSCs was significantly different or not. The p value was 0.0788 when we compared the three wild-type with *Mrg15* null clones, and close to significance. This was because one of the *Mrg15* deficient NSC clones had relatively lower expression of p21 (Fig 1A). However, if this clone was removed from the analysis the p value was highly significant 0.0005. It appears that about 10% of the NSC clones do not show p21 upregulation though they still exhibit a growth defect, suggesting the existence of a p21 independent mechanism for growth defect observed.

We then determined the expression levels of p16INK4a (Fig. 1B) and p19ARF (Fig. 1C) by qRT-PCR, since these other cell cycle regulators have been shown to be important in stem cell self-renewal [51–53]. We did not find any correlation between their expression and the cell growth defect of *Mrg15* deficient NSC cultures. p16 and p19 expression levels were not statistically significantly different between wild-type and *Mrg15* deficient NSCs.

We also determined p21 protein levels in wild-type and *Mrg15* deficient neurosphere cultures by Western blot. As expected, p21 protein expression was upregulated in early passage of *Mrg15* deficient but not wild-type neurosphere cultures (Fig. 2 **upper panel**) and the difference was statistically different (p value 0.0085, unpaired t test). This suggests that p21 upregulation in *Mrg15* deficient NSCs is caused by transcriptional activation of p21 gene. Interestingly, p21 expression was also upregulated in later passage (6th) wild-type neurosphere cultures (Fig. 2 **lower panel**), at which time these cultures also exhibited slow growth.

### Downregulation of p21 expression improves cell growth in *Mrg15* deficient NSCs

To determine whether p21 is an active regulatory gene in the growth defect of *Mrg15* deficient NSCs, we performed p21 knockdown in these cells and examined the rate of BrdU incorporation. Because p21 expression was also upregulated in late passage of wild-type NSC cultures which showed slow growth, we compared the effect of p21 knockdown in first passage cultures of *Mrg15* deficient NSCs with that of late passage (6th) cultures of wild-type cells. We used a lentivirus shRNA expression system for this purpose because p21 knockdown occurred efficiently [48, 49] and siRNA transfection using liposomes was highly toxic to the NSCs. Knockdown of p21 following infection with a lentivirus



expressing p21 shRNA occurred efficiently (>80%) in both *Mrg15* deficient and wild-type NSCs (Fig. 3A) as described previously [48]. Infection efficiency of lentivirus, as indicated by GFP expression, was not different between *Mrg15* deficient and wild-type NSCs or empty vector and p21 shRNA constructs. Knockdown of p21 in *Mrg15* deficient NSCs significantly increased BrdU incorporation (from 24% to 36%) (Fig. 3B). This result indicates that upregulation of p21 expression contributes to the growth defect in *Mrg15* deficient NSCs. Late passage wild-type NSC cultures also had a reduced rate of BrdU incorporation (26%), which corresponded with slow growth, and knockdown of p21 improved BrdU incorporation (45%) (Fig. 3C). This suggests that p21 is a critical regulator for passage-dependent growth regulation in NSCs. The effect of p21 knockdown in *Mrg15* deficient NSCs was less than that in late passage wild-type NSCs indicating that other molecular mechanisms may exist for the observed growth defects in *Mrg15* deficient NSCs, in addition to p21 up-regulation.

We further confirmed the effect of p21 knockdown on cell cycle distribution in early passage *Mrg15* deficient NSCs and 6th passage wild-type NSCs using FACS. Similar to the BrdU incorporation results, the S phase population significantly increased in both *Mrg15* deficient and wild-type NSCs after infection with lentivirus expressing p21 shRNA (Fig. 3E and G) when compared with that of cells infected with lentivirus containing the empty vector (Fig. 3D and F).

We have previously shown that nestin positive cell populations in *Mrg15* deficient NSC cultures was almost the same as that of wild-type cultures [46]. This suggests that the growth defect caused by p21 upregulation in *Mrg15* deficient NSC cultures most likely occurs in stem/progenitor populations and that these are not increased by spontaneous differentiation in growth medium.

### **P53 is activated in *Mrg15* deficient NSCs**

It is well known that p21 expression is transcriptionally regulated by the tumor suppressor gene p53. p53 is activated by phosphorylation and acetylation in response to internal and external stresses such as exposure to radiation, and activated p53 upregulates expression of target genes, including p21. Therefore, we analyzed *Mrg15* deficient versus wild-type NSCs for expression of the activated form of p53, using an anti-phosphorylated p53Ser15 (Ser18 in mouse) antibody, by Western blot (Fig. 4A). A higher amount of activated p53 accumulated in *Mrg15* deficient NSC cultures compared with that in wild-type cultures, except in the case of one clone of the 5 analyzed. When this clone was eliminated from analysis the higher levels were significant, p value 0.0132. Levels of p21 expression co-related with accumulation of activated p53. We also confirmed complete loss of *Mrg15* expression in *Mrg15* deficient NSCs.

We used a lentivirus encoding p53 shRNA [50] and an empty vector control to perform studies similar to those done with p21, described above. Down-regulation of p53 in *Mrg15* deficient NSCs was confirmed by Western analyses (Fig. 4B). BrdU incorporation indicated an increase in positive cells following p53 knockdown in *Mrg15* deficient cells (Fig. 4C) and p21 positively stained cells were decreased (Fig. 4D). This suggests that p53 is activated and accumulates in *Mrg15* deficient NSCs and this in turn upregulates p21 expression.

### **DNA damage foci are detected in *Mrg15* deficient NSC cultures and are present in p21 positive cells**

p53 is activated in response to intrinsic and extrinsic stimuli such as DNA damage. Because activated p53 accumulates in *Mrg15* deficient NSC cultures, we examined whether there is more DNA damage in *Mrg15* deficient NSC cultures compared with wild-type. We detected

foci for  $\gamma$ H2AX and 53BP1 in nuclei using immunocytochemistry, because these two proteins form foci at damage sites in DNA. Although we could not easily find focus positive cells in wild-type NSC cultures (Fig. 5A, **upper panels**), focus positive cells were easily detectable in *Mrg15* deficient NSC cultures without any stress insults (Fig. 5A, **lower panels**). The focus number in *Mrg15* deficient NSCs was usually less than 10 foci in each nucleus under normal culture condition but the majority of these foci was  $\gamma$ H2AX and 53BP1 double positive. This result suggests that DNA damage accumulates in *Mrg15* deficient NSC cultures versus wild-type NSC cultures under growing conditions.

p21 expression is upregulated by activated p53 after DNA damage and involved in cell cycle arrest to repair damaged DNA in cells. To examine whether accumulation of p21 in *Mrg15* deficient NSCs is caused by DNA damage response, we performed co-immunostaining with anti-p21 and anti-53BP1 antibodies (Fig. 5B). p21-positive staining was observed in *Mrg15* deficient NSC cultures but not in early passage wild-type NSC cultures (Fig. 5C). The majority of p21 positive cells in *Mrg15* deficient NSC cultures was also 53BP1 focus positive ( $62.5 \pm 7.6\%$ , Mean  $\pm$  SEM, n=12 fields), whereas we could not detect 53BP1 foci in early passage wild-type NSC cultures. We did not detect 53BP1 foci in about 30–35% of p21 positive cells of in *Mrg15* deficient NSCs. Thus, p21 accumulation in these cells may occur via DNA damage independent regulation.

### Defects of DNA damage response in *Mrg15* deficient NSCs

The results described above suggest that MRG15 is critical for DNA damage repair in NSCs. We therefore examined the DNA damage response of *Mrg15* deficient NSCs compared with that of wild-type NSCs. *Mrg15* deficient and wild-type NSCs were subjected to  $\gamma$ -irradiation at 10 Gy and focus formation of 53BP1 and  $\gamma$ H2AX at indicated time points was measured by immunostaining. As expected, foci for  $\gamma$ H2AX and 53BP1 were easily detected at all time points except for 0 time point after irradiation in wild-type NSCs (Fig. 6A). In *Mrg15* deficient NSCs, some cells already had small but detectable foci for  $\gamma$ H2AX and 53BP1 at the 0 time point (less than 10 foci per nucleus, corresponding to baseline level). Although we could detect focus formation of these in *Mrg15* deficient NSCs in response to  $\gamma$ -irradiation, focus formation for both  $\gamma$ H2AX and 53BP1 was significantly delayed and foci of these were usually smaller compared with those in wild-type NSCs (Fig. 6B, C and D). This result showed that *Mrg15* deficient NSCs have defects in the DNA damage response and this could result in inefficient DNA repair. This inefficient DNA damage response may explain partly explain the growth defect of *Mrg15* deficient NSCs in growing conditions.

It has been reported that MRG15 directly interacts with PALB2 and is involved in DNA damage repair by homologous recombination (HR) after IR [54, 55]. Next, we examined whether RAD51 focus formation after IR was affected by *Mrg15* deficiency using immunostaining. RAD51 foci were negative in almost all cells in both genotypes without IR, although a few cells had one or two very small foci (less than 5 foci in the nucleus). About 30% of wild-type NSCs had RAD51 foci at 3 h after IR (Fig. 7A and C). However, only 7% of *Mrg15* deficient NSCs had RAD51 foci at the same time point after IR (Fig. 7B and C). Western analysis revealed no significant difference in total protein levels of RAD51 in wild-type versus *Mrg15* deficient cells (Fig. 7D). However, it is focus formation that is the critical response suggesting that MRG15 is also important for RAD51 recruitment at the damage sites after DNA damage and may affect homologous recombination dependent DNA damage repair as well as DNA damage response in NSCs.

## DISCUSSION

Chromatin regulation is involved in DNA replication, transcriptional regulation and DNA damage repair and is a crucial step for stem cell self-renewal and function. We had previously shown that inactivation of the chromatin regulator MRG15 impairs proliferation of embryonic NSCs. In this report, we demonstrate that this occurs through activation of p53 and resulting increased expression of the cdk inhibitor p21. We have found increased expression of p21 and activated p53 in primary cell cultures of *Mrg15* null NSCs but not wild-type. Focus formation of 53BP1, which indicates the presence of DNA damage, also co-localizes with p21 in *Mrg15* null NSCs in growing culture condition, without any extrinsic insults. Focus formation of 53BP1 after  $\gamma$ -irradiation is delayed in *Mrg15* null NSCs compared with wild-type NSCs. Our observations suggest that chromatin regulation and DNA damage repair through MRG15 complex(es) is essential to establish and maintain a functional NSC pool in mouse brain during development.

Maintenance of genomic integrity is important for stem cell function in various stem cells including NSCs [56–58]. Perturbations in genes involved in DNA damage response signaling pathways and/or DNA repair are associated with neurological disorders such as neurodegeneration, microcephaly and brain tumors, suggesting that the inability to respond to DNA damage interferes with normal tissue homeostasis [58–60]. DNA damage response and repair are critical for stem/progenitor cell amplification and ensure the establishment of a functional nervous system. Mice deficient for any one of the many genes that play a role in the cellular response to DNA damage (*Atm*, *Mre11*, *Nbs1*) [61–64] or genes actively involved in DNA repair (*BRCA2* and *Lig4*) [65–67] all share a phenotype of neurological failure due to defective DNA damage repair. These deletions affect NSC self-renewal as well as neuronal function.

MRG15 is involved in DNA damage repair [42, 44] in addition to transcriptional regulation of cell proliferation [47]. Thus there are two possibilities to explain the molecular mechanism by which MRG15 could be involved in the proliferative defects in *Mrg15* null NSCs that we have observed. These are via the Tip60 complex or the PALB2/*BRCA2* interaction involving MRG15. In *Drosophila*, the Tip60 complex acetylates nucleosomal phospho-H2Av, a *Drosophila* H2AX homolog, in response to ionizing radiation and exchanges it with an unmodified H2Av [42] and knockdown of either dTip60 or dMrg15 in *Drosophila* cells impaired this acetylation and exchange of H2Av following irradiation. In mammalian cells, depletion of either Tip60 or TRRAP, other components of the Tip60 complex, results in impairment of recruitment of DNA-repair proteins such as 53BP1 to damage sites [43]. The Tip60/TRRAP complex acetylates histone H2A and H2AX at DNA damage sites and thereby maintains open chromatin and facilitates access of DNA repair machinery to DNA strand break sites. Ikura et. al showed that H2AX acetylated by Tip60 after ionizing radiation leads to ubiquitination by DNA damage induced UBC13[45]. Tip60 promotes the acetylation-dependent ubiquitination of H2AX by UBC13, causing H2AX release from chromatin and thereby facilitates chromatin reorganization following DNA damage. We have also shown that acetylation of histone H2A, in response to ionizing radiation (IR), is impaired and recruitment of DNA repair proteins delayed in *Mrg15* null MEFs [44]. Because the Tip60 complex is important for self-renewal of embryonic stem (ES) cells [68, 69], the role of MRG15 in proliferation defects of NSC may also occur via the Tip60 complex.

Another possible connection between MRG15 and DNA damage is PALB2. PALB2 was originally identified as an interacting partner of *BRCA2* which is a tumor suppressor for breast and ovarian cancers and is required for the loading of the *BRCA2*-*RAD51* repair complex onto DNA. More recently, it was shown that PALB2 can also bind to *BRCA1* and



that it is an integral component of the BRCA1-BRCA2-RAD51 axis, which is critical for the maintenance of genomic stability via recombinational repair. Two groups have shown that MRG15 can bind directly to PALB2 and that knockdown of MRG15 affects homology-directed DNA repair [54, 55], although results from these reports are contradictory. Sy and co-workers showed that PALB2-deficient EUF1341F cells reconstituted with MRG15-binding defective PALB2 mutant exhibited increased gene conversion rates although damage-induced RAD51 foci formation and mitomycin C sensitivity returned to normal in this cells. This suggests MRG15 inhibits homologous recombination through PALB2 interaction. On the other hand, Hayakawa and coworkers demonstrated that MRG15 deficient cells showed reduced efficiency for homology-directed DNA repair and hypersensitivity to DNA interstrand cross-linking agents similar to PALB2 or BRCA2 deficient cells. They also showed that MRG15 knockdown diminished the recruitment of PALB2, BRCA2, and RAD51 to DNA damage sites. Although we do understand this discrepancy, our previous and current findings support the fact that MRG15 is an essential factor for DNA damage repair in somatic cells as well as stem cells. Deletion of *Brca2* in the entire nervous system in mice leads to microcephaly and defects in neurogenesis [67]. p53 contributes to these phenotypes because simultaneous inactivation of p53 improves *Brca2* depletion phenotypes in mouse brains. p53 is responsible for both cell growth defect and apoptosis in *Brca2*-deficient NSCs. MRG15 may therefore also function through a BRCA2 pathway in NSCs.

The tumor suppressor p53 is an important regulator of cell cycle and apoptosis in both developing and adult brain and plays an important role in maintaining a proper balance of neural stem/progenitor pools. It is known that one of the p53 downstream target genes, p21, is also important for maintaining NSC self-renewal during the lifespan of an organism [70, 71]. In the absence of p53, NSCs isolated from adult mice as well as mouse embryos exhibit a higher proliferation rate in culture [72–74]. On the other hand, p44Tg mice, in which p53 is constitutively activated, exhibit premature aging without increased tumor risk, indicating that constitutive activation of p53 limits NSC self-renewal following constitutive expression of p21 [75, 76]. Therefore, it is possible that p53 activation following increased p21 expression may limit self-renewal potential in *Mrg15* deficient NSCs. This is supported by the fact that knockdown of p53 levels results in decreased p21 expression and an increase in BrdU-positive cycling cells in both wild-type and *Mrg15* null cells, as shown in this study. It is known that p53 also inhibits neuronal differentiation because p53 deficient NSCs differentiate into neuronal lineage in higher rate [73, 77]. We have previously shown *Mrg15* deficient NSCs had a defect in neuronal differentiation. This defect may also be explained by upregulation of p53 activity in *Mrg15* deficient NSCs.

Epigenetic mechanisms are essential for normal brain development and function and dysregulation in chromatin regulation results in neurodegenerative disorders, such as Alzheimer disease [78]. It has been shown that expression of cell cycle-related proteins increases in the degenerating neurons in Alzheimer disease and re-entry into the cell cycle in neurons occurs aberrantly [79–81]. Because MRG15 is involved in cell cycle regulation through chromatin regulation, dysregulation of MRG15 may contribute to the initiation and/or progression of such neurodegenerative disorders.

Our knowledge of the many functions of MRG15 continues to expand. We have determined that some of the major functions of MRG15 include transcriptional regulation via complexes involving both HATs and HDACs. Although we here demonstrate the importance of MRG15 in NSC proliferation through a DNA damage response, we speculate that other molecular mechanisms are also involved. MRG15 may directly modulate expression of genes that are important for cell cycle regulation. A small percentage of *Mrg15* deficient NSCs did not show DNA damage foci, although p21 was overexpressed in these cells.

MRG15 is a component of mSin3/HDAC1/Pf1 complex and it has been shown that this complex has a transcriptional repressor activity [29, 34]. Although this complex is mainly recruited into coding regions of actively expressing genes, which are marked by trimethylation of histone H3 at lysine 36, to prevent uncontrolled chromatin relaxation downstream of the transcriptional start sites [82], it remains possible that this complex repressively modulates the promoter activity of specific genes such as p21. In fact, it has been shown that MRGX, MRG15 homolog, also has a transcriptional repressor activity depending on the cell-type analyzed [83]. p21 expression may be repressed by a MRG15-containing repressor complex in wild-type NSCs under normal conditions and p21 accumulation in *Mrg15* deficient NSCs may occur through de-repression of this promoter activity in a DNA damage independent manner. This possibility is currently being explored. It may also be possible that MRG15 negatively controls p21 expression via the Tip60/p400 complex, of which MRG15 is a component [84–86]. Additional studies are required to determine the complexity of the molecular mechanisms involved.

## Conclusions

Our study demonstrates a critical role of the chromatin regulator MRG15 in proliferation of NSCs in vitro. Loss of *Mrg15* in NSCs shows increased 53BP1 focus formation, activated p53, and a resulting increase in p21. This suggests that maintenance of genomic integrity through chromatin regulation is essential to establish a functional nervous system. This study should provide insights into the molecular mechanism(s) involved in chromatin regulation in NSC self-renewal and function in the mouse brain.

## Acknowledgments

We thank Drs. Timothy N. Phoenix and Sally Temple and Dr. Tomoo Iwakuma for providing lentivirus vectors for p21 shRNA and p53 shRNA (pSicoR p53) and technical advice. We also thank Dr. Benjamin J. Daniel for FACS analyses and Mrs. Emiko Tominaga for some experiments. This study was supported by funding from NIH/NIA RO1AG032134 and SALSI to OMPS and American Heart Association grant 0765084Y to KT.

## The abbreviations used are

<b>MRG15</b>	MORF4 related factor on human chromosome 15
<b>HAT</b>	histone acetyltransferase
<b>HDAC</b>	histone deacetylase
<b>NSCs</b>	neural stem/progenitor cells
<b>IR</b>	ionizing radiation
<b>DSBs</b>	DNA double strand breaks

## References

1. Gage FH. Mammalian neural stem cells. *Science*. 2000; 287:1433–1438. [PubMed: 10688783]
2. Temple S. The development of neural stem cells. *Nature*. 2001; 414:112–117. [PubMed: 11689956]
3. Shi Y, Sun G, Zhao C, Stewart R. Neural stem cell self-renewal. *Crit Rev Oncol Hematol*. 2008; 65:43–53. [PubMed: 17644000]
4. Ma DK, Bonaguidi MA, Ming G-L, Song H. Adult neural stem cells in the mammalian central nervous system. *Cell Res*. 2009; 19:672–682. [PubMed: 19436263]
5. Reynolds BA, Weiss S. Generation of neurons and astrocytes from isolated cells of the adult mammalian central nervous system. *Science*. 1992; 255:1707–1710. [PubMed: 1553558]

6. Reynolds BA, Weiss S. Clonal and population analyses demonstrate that an EGF-responsive mammalian embryonic CNS precursor is a stem cell. *Dev Biol.* 1996; 175:1–13. [PubMed: 8608856]
7. Borrelli E, Nestler EJ, Allis CD, Sassone-Corsi P. Decoding the epigenetic language of neuronal plasticity. *Neuron.* 2008; 60:961–974. [PubMed: 19109904]
8. Li X, Zhao X. Epigenetic regulation of mammalian stem cells. *Stem Cells Dev.* 2008; 17:1043–1052. [PubMed: 18393635]
9. Mehler MF. Epigenetics and the nervous system. *Ann Neurol.* 2008; 64:602–617. [PubMed: 19107999]
10. Wen S, Li H, Liu J. Epigenetic background of neuronal fate determination. *Prog Neurobiol.* 2009; 87:98–117. [PubMed: 19007844]
11. Hsieh J, Eisch AJ. Epigenetics, hippocampal neurogenesis, and neuropsychiatric disorders: unraveling the genome to understand the mind. *Neurobiol Dis.* 2010 in press.
12. Penner MR, Roth TL, Barnes CA, Sweatt JD. An epigenetic hypothesis of aging-related cognitive dysfunction. *Front Aging Neurosci.* 2010; 2:9. [PubMed: 20552047]
13. Lim DA, Huang YC, Swigut T, Mirick AL, Garcia-Verdugo JM, Wysocka J, Ernst P, Alvarez-Buylla A. Chromatin remodelling factor Mll1 is essential for neurogenesis from postnatal neural stem cells. *Nature.* 2009; 458:529–533. [PubMed: 19212323]
14. Wang J, Weaver ICG, Gauthier-Fisher A, Wang H, He L, Yeomans J, Wondisford F, Kaplan DR, Miller FD. CBP histone acetyltransferase activity regulates embryonic neural differentiation in the normal and Rubinstein-Taybi syndrome brain. *Dev Cell.* 2010; 18:114–125. [PubMed: 20152182]
15. Peleg S, Sananbenesi F, Zovoilis A, Burkhardt S, Bahari-Javan S, Agis-Balboa RC, Cota P, Wittnam JL, Gogol-Doering A, Opitz L, Salinas-Riester G, Dettenhofer M, Kang H, Farinelli L, Chen W, Fischer A. Altered histone acetylation is associated with age-dependent memory impairment in mice. *Science.* 2010; 328:753–756. [PubMed: 20448184]
16. Guan J-S, Haggarty SJ, Giacometti E, Dannenberg J-H, Joseph N, Gao J, Nieland TJ, Zhou Y, Wang X, Mazitschek R, Bradner JE, DePinho RA, Jaenisch R, Tsai L-H. HDAC2 negatively regulates memory formation and synaptic plasticity. *Nature.* 2009; 459:55–60. [PubMed: 19424149]
17. Bertram MJ, Berube NG, Hang-Swanson X, Ran Q, Leung JK, Bryce S, Spurgers K, Bick RJ, Baldini A, Ning Y, Clark LJ, Parkinson EK, Barrett JC, Smith JR, Pereira-Smith OM. Identification of a gene that reverses the immortal phenotype of a subset of cells and is a member of a novel family of transcription factor-like genes. *Mol Cell Biol.* 1999; 19:1479–1485. [PubMed: 9891081]
18. Marin I, Baker BS. Origin and evolution of the regulatory gene *male-specific lethal-3*. *Mol Biol Evol.* 2000; 17:1240–1250. [PubMed: 10908644]
19. Bertram MJ, Pereira-Smith OM. Conservation of the *MORF4 related* gene family: identification of a new chromo domain subfamily and novel protein motif. *Gene.* 2001; 266:111–121. [PubMed: 11290425]
20. Cavalli G, Paro R. Chromo-domain proteins: linking chromatin structure to epigenetic regulation. *Curr Opin Cell Biol.* 1998; 10:354–360. [PubMed: 9640536]
21. Jones DO, Cowell IG, Singh PB. Mammalian chromodomain proteins: their role in genome organisation and expression. *Bioessays.* 2000; 22:124–137. [PubMed: 10655032]
22. Brehm A, Tufteland KR, Aasland R, Becker PB. The many colours of chromodomain. *Bioessays.* 2004; 26:133–140. [PubMed: 14745831]
23. Joshi AA, Struhl K. Eaf3 chromodomain interaction with methylated H3-K36 links histone deacetylation to Pol II elongation. *Mol Cell.* 2005; 20:971–978. [PubMed: 16364921]
24. Zhang P, Du J, Sun B, Dong X, Xu G, Zhou J, Huang Q, Liu Q, Hao Q, Ding J. Structure of human MRG15 chromo domain and its binding to Lys36-methylated histone H3. *Nucleic Acids Res.* 2006; 34:6621–6628. [PubMed: 17135209]
25. Sun B, Hong J, Zhang P, Dong X, Shen X, Lin D, Ding J. Molecular basis of the interaction of *Saccharomyces cerevisiae* Eaf3 chromo domain with methylated H3K36. *J Biol Chem.* 2008; 283:36504–36512. [PubMed: 18984594]

26. Ikura T, Ogryzko VV, Grigoriev M, Groisman R, Wang J, Horikoshi M, Scully R, Qin J, Nakatani Y. Involvement of the TIP60 histone acetylase complex in DNA repair and apoptosis. *Cell*. 2000; 102:463–473. [PubMed: 10966108]
27. Eisen A, Utley RT, Nourani A, Allard S, Schmidt P, Lane WS, Lucchesi JC, Cote J. The yeast NuA4 and *Drosophila* MSL complexes contain homologous subunits important for transcription regulation. *J Biol Chem*. 2001; 276:3484–3491. [PubMed: 11036083]
28. Pardo PS, Leung JK, Lucchesi JC, Pereira-Smith OM. MRG15 a novel chromodomain protein is present in two distinct multiprotein complexes involved in transcriptional activation. *J Biol Chem*. 2002; 277:50860–50866. [PubMed: 12397079]
29. Yochum GS, Ayer DE. Role for the mortality factors MORF4, MRGX, and MRG15 in transcriptional repression via associations with Pf1, mSin3A. *Mol Cell Biol*. 2002; 22:7868–7876. [PubMed: 12391155]
30. Cai Y, Jin J, Tomomori-Sato C, Sato S, Sorokina I, Parmely TJ, Conaway RC, Conaway JW. Identification of new subunits of the multiprotein mammalian TRRAP/TIP60-containing histone acetyltransferase complex. *J Biol Chem*. 2003; 278:42733–42736. [PubMed: 12963728]
31. Doyon Y, Selleck W, Lane WS, Tan S, Cote J. Structural and functional conservation of the NuA4 histone acetyltransferase complex from yeast to humans. *Mol Cell Biol*. 2004; 24:1884–1896. [PubMed: 14966270]
32. Doyon Y, Cote J. The highly conserved and multifunctional NuA4 complex. *Curr Opin Genet Dev*. 2004; 14:147–154. [PubMed: 15196461]
33. Doyon Y, Cayrou C, Ullah M, Landry A-J, Cote V, Selleck W, Lane WS, Tan S, Yang X-J, Cote J. ING tumor suppressor proteins are critical regulators of chromatin acetylation required for genome expression and perpetuation. *Mol Cell*. 2006; 21:51–64. [PubMed: 16387653]
34. Hayakawa T, Ohtani Y, Hayakawa N, Shinmyozu K, Saito M, Ishikawa F, Nakayama J. RBP2 is an MRG15 complex component and down-regulates intragenic histone H3 lysine 4 methylation. *Genes Cells*. 2007; 12:811–826. [PubMed: 17573780]
35. Sardi ME, Cai Y, Jin J, Swanson SK, Conaway RC, Conaway JW, Florens L, Washburn MP. Probabilistic assembly of human protein interaction networks from label-free quantitative proteomics. *Proc Natl Acad Sci USA*. 2008; 105:1454–1459. [PubMed: 18218781]
36. Lee N, Erdjument-Bromage H, Tempst P, Jones RS, Zhang Y. The H3K4 demethylase Lid associates with and inhibits histone deacetylase Rpd3. *Mol Cell Biol*. 2009; 29:1401–1410. [PubMed: 19114561]
37. Moshkin YM, Kan TW, Goodfellow H, Bezstarosti K, Maeda RK, Pilyugin M, Karch F, Bray SJ, Demmers JA, Verrijzer CP. Histone chaperones ASF1 and NAP1 differentially modulate removal of active histone marks by LID-RPD3 complexes during NOTCH silencing. *Mol Cell*. 2009; 35:782–793. [PubMed: 19782028]
38. Carrozza MJ, Li B, Florens L, Sukanuma T, Swanson SK, Lee KK, Shia W-J, Anderson S, Yates J, Washburn MP, Workman JL. Histone H3 methylation by Set2 directs deacetylation of coding regions by Rpd3S to suppress spurious intragenic transcription. *Cell*. 2005; 123:581–592. [PubMed: 16286007]
39. Keogh M-C, Kurdistani SK, Morris SA, Ahn SH, Podolny V, Collins SR, Schuldiner M, Chin K, Punna T, Thompson NJ, Boone C, Emili A, Weissman JS, Hughes TR, Strahl BD, Grunstein M, Greenblatt JF, Buratowski S, Krogan NJ. Cotranscriptional Set2 methylation of histone H3 lysine 36 recruits a repressive Rpd3 complex. *Cell*. 2005; 123:593–605. [PubMed: 16286008]
40. Nicolas E, Yamada T, Cam HP, FitzGerald PC, Kobayashi R, Grewal SIS. Distinct roles of HDAC complexes in promoter silencing, antisense suppression and DNA damage protection. *Nat Struct Mol Biol*. 2007; 14:372–380. [PubMed: 17450151]
41. Squatrito M, Gorrini C, Amati B. Tip60 in DNA damage response and growth control: many tricks in one HAT. *Trends Cell Biol*. 2006; 16:433–442. [PubMed: 16904321]
42. Kusch T, Florens L, MacDonald WH, Swanson SK, Glaser RL, Yates JR III, Abmayr SM, Washburn MP, Workman JL. Acetylation by Tip60 is required for selective histone variant exchange at DNA lesions. *Science*. 2004; 306:2084–2087. [PubMed: 15528408]

43. Murr R, Loizou JI, Yang Y-G, Cuenin C, Li H, Wang Z-Q, Herceg Z. Histone acetylation by Trrap-Tip60 modulates loading of repair proteins and repair of DNA double-strand breaks. *Nat Cell Biol.* 2006; 8:91–99. [PubMed: 16341205]
44. Garcia SN, Kirtane BM, Podlutzky AJ, Pereira-Smith OM, Tominaga K. *Mrg15* null and heterozygous mouse embryonic fibroblasts exhibit DNA-repair defects post exposure to gamma ionizing radiation. *FEBS Lett.* 2007; 581:5275–5281. [PubMed: 17961556]
45. Ikura T, Tashiro S, Kakino A, Shima H, Jacob N, Amunugama R, Yoder K, Izumi S, Kuraoka I, Tanaka K, Kimura H, Ikura M, Nishikubo S, Ito T, Muto A, Miyagawa K, Takeda S, Fishel R, Igarashi K, Kamiya K. DNA damage-dependent acetylation and ubiquitination of H2AX enhances chromatin dynamics. *Mol Cell Biol.* 2007; 27:7028–7040. [PubMed: 17709392]
46. Chen M, Takano-Maruyama M, Pereira-Smith OM, Gaufo GO, Tominaga K. MRG15, a component of HAT and HDAC complexes, is essential for proliferation and differentiation of neural precursor cells. *J Neurosci Res.* 2009; 87:1522–1531. [PubMed: 19115414]
47. Tominaga K, Kirtane B, Jackson JG, Ikeno Y, Ikeda T, Hawks C, Smith JR, Matzuk MM, Pereira-Smith OM. MRG15 regulates embryonic development and cell proliferation. *Mol Cell Biol.* 2005; 25:2924–2937. [PubMed: 15798182]
48. Fasano CA, Dimos JT, Ivanova NB, Lowry N, Lemischka IR, Temple S. shRNA knockdown of Bmi-1 reveals a critical role for p21-Rb pathway in NSC self-renewal during development. *Cell Stem Cell.* 2007; 1:87–99. [PubMed: 18371338]
49. Phoenix TN, Temple S. Spred1, a negative regulator of Ras-MAPK-ERK, is enriched in CNS germinal zones, dampens NSC proliferation, and maintains ventricular zone structure. *Genes Dev.* 2010; 24:45–56. [PubMed: 20047999]
50. Ventura A, Meissner A, Dillon CP, McManus M, Sharp PA, Van Parijs L, Jaenisch R, Jacks T. Cre-lox-regulated conditional RNA interference from transgenes. *Proc Natl Acad Sci USA.* 2004; 101:10380–10385. [PubMed: 15240889]
51. Jacobs JLL, Kieboom K, Marino S, DePinho RA, van Lohuizen M. The oncogene and polycomb-group gene *bmi-1* regulates cell proliferation and senescence through the *ink4a* locus. *Nature.* 1999; 397:164–168. [PubMed: 9923679]
52. Molofsky AV, Slutsky SG, Joseph NM, He S, Pardal R, Krishnamurthy J, Sharpless NE, Morrison SJ. Increasing p16INK4a expression decreases forebrain progenitors and neurogenesis during ageing. *Nature.* 2006; 443:448–452. [PubMed: 16957738]
53. Nishino J, Kim I, Chada K, Morrison SJ. Hmga2 promotes neural stem cell self-renewal in young but not old mice by reducing p16Ink4a and p19Arf expression. *Cell.* 2008; 135:227–239. [PubMed: 18957199]
54. Sy SM-H, Huen MS, Chen J. MRG15 is a novel PALB2-interacting factor involved in homologous recombination. *J Biol Chem.* 2009; 284:21127–21131. [PubMed: 19553677]
55. Hayakawa T, Zhang F, Hayakawa N, Ohtani Y, Shinmyozu K, Nakayama J, Andreassen PR. MRG15 binds directly to PALB2 and stimulates homology-directed repair of chromosomal breaks. *J Cell Sci.* 2010; 123:1124–1130. [PubMed: 20332121]
56. Nijnik A, Woodbine L, Marchetti C, Dawson S, Lambe T, Liu C, Rodrigues NP, Crockford TL, Cabuy E, Vindigni A, Enver T, Bell JI, Slijepcevic P, Goodnow CC, Jeggo PA, Cornall RJ. DNA repair is limiting for haematopoietic stem cells during ageing. *Nature.* 2007; 447:686–690. [PubMed: 17554302]
57. Rossi DJ, Bryder D, Seita J, Nussenzweig A, Hoeijmakers J, Weissman IL. Deficiencies in DNA damage repair limit the function of haematopoietic stem cells with age. *Nature.* 2007; 447:725–729. [PubMed: 17554309]
58. McKinnon PJ. DNA repair deficiency and neurological disease. *Nat Rev Neurosci.* 2009; 10:100–112. [PubMed: 19145234]
59. Lee Y, Mckinnon PJ. Responding to DNA double strand breaks in the nervous system. *Neuroscience.* 2007; 145:1365–1374. [PubMed: 16934412]
60. Frappart P-O, McKinnon PJ. Mouse models of DNA double-strand break repair and neurological disease. *DNA Repair.* 2008; 7:1051–1060. [PubMed: 18458002]
61. Stewart GS, Maser RS, Stankovic T, Bressan DA, Kaplan MI, Jaspers NG, Raams A, Byrd PJ, Petrini JH, Taylor AM. The DNA double-strand break repair gene hMRE11 is mutated in



- individuals with an ataxia-telangiectasia-like disorder. *Cell*. 1999; 99:577–587. [PubMed: 10612394]
62. Allen DM, van Praag H, Ray J, Weaver Z, Winrow CJ, Carter TA, Braquet R, Harrington E, Ried T, Brown KD, Gage FH, Barlow C. Ataxia telangiectasia mutated is essential during adult neurogenesis. *Genes Dev*. 2001; 15:554–566. [PubMed: 11238376]
  63. Frappart P-O, Tong W-M, Demuth I, Radovanovic I, Herceg Z, Aguzzi A, Digweed M, Wang Z-Q. An essential function for NBS1 in the prevention of ataxia and cerebellar defects. *Nat Med*. 2005; 11:538–544. [PubMed: 15821748]
  64. Shull ERP, Lee Y, Nakane H, Stracker TH, Zhao J, Russell HR, Petrini JHJ, McKinnon PJ. Differential DNA damage signaling accounts for distinct neural apoptotic responses in ATLD and NBS. *Genes Dev*. 2009; 23:171–180. [PubMed: 19171781]
  65. Lee Y, Barnes DE, Lindahl T, McKinnon PJ. Defective neurogenesis resulting from DNA ligase IV deficiency requires Atm. *Genes Dev*. 2000; 14:2576–2580. [PubMed: 11040211]
  66. O'Driscoll M, Cerosaletti KM, Girard P-M, Dai Y, Stumm M, Kysela B, Hirsch B, Gennery A, Palmer SE, Seidel J, Gatti RA, Varon R, Oettinger MA, Neitzel H, Jeggo PA, Concannon P. DNA ligase IV mutations identified in patients exhibiting developmental delay and immunodeficiency. *Mol Cell*. 2001; 8:1175–1185. [PubMed: 11779494]
  67. Frappart P-O, Lee Y, Lamont J, McKinnon PJ. BRCA2 is required for neurogenesis and suppression of medulloblastoma. *EMBO J*. 2007; 26:2732–2742. [PubMed: 17476307]
  68. Fazio TG, Huff JT, Panning B. An RNAi screen of chromatin proteins identifies Tip60- p400 as a regulator of embryonic stem cell identity. *Cell*. 2008; 134:162–174. [PubMed: 18614019]
  69. Fazio TG, Huff JT, Panning B. Chromatin regulation Tip(60)s the balance in embryonic stem cell self-renewal. *Cell Cycle*. 2008; 7:3302–3306. [PubMed: 18948739]
  70. Kippin TE, Martens DJ, van der Kooy D. p21 loss compromises the relative quiescence of forebrain stem cell proliferation leading to exhaustion of their proliferation capacity. *Genes Dev*. 2005; 19:756–767. [PubMed: 15769947]
  71. Pechnick RN, Zonis S, Wawrowsky K, Pourmorady J, Chesnokova V. p21Cip1 restricts neuronal proliferation in the subgranular zone of the dentate gyrus of the hippocampus. *Proc Natl Acad Sci USA*. 2008; 105:1358–1363. [PubMed: 18172194]
  72. Gil-Perotin S, Marin-Husstege M, Li J, Soriano-Navarro M, Zindy F, Roussel MF, Garcia-Verdugo JM, Casaccia-Bonnel P. Loss of p53 induces changes in the behavior of subventricular zone cells: implication for the genesis of glial tumors. *J Neurosci*. 2006; 26:1107–1116. [PubMed: 16436596]
  73. Meletis K, Wirta V, Hede SM, Nister M, Lundberg J, Frisen J. p53 suppresses the self-renewal of adult neural stem cells. *Development*. 2006; 133:363–369. [PubMed: 16368933]
  74. Armesilla-Diaz A, Bragado P, Del Valle I, Cuevas E, Lazaro I, Martin C, Cigudosa JC, Silva A. p53 regulates the self-renewal and differentiation of neural precursors. *Neuroscience*. 2009; 158:1378–1389. [PubMed: 19038313]
  75. Medrano S, Scrabble H. Maintaining appearances-the role of p53 in adult neurogenesis. *Biochem Biophys Res Commun*. 2005; 331:828–833. [PubMed: 15865938]
  76. Medrano S, Burns-Cusato M, Atienza MB, Rahimi D, Scrabble H. Regenerative capacity of neural precursors in the adult mammalian brain is under the control of p53. *Neurobiol Aging*. 2009; 30:483–497. [PubMed: 17850928]
  77. Ferron SR, Marques-Torres MA, Mira H, Flores I, Taylor K, Blasco MA, Farinas I. Telomere shortening in neural stem cells disrupts neuronal differentiation and neurogenesis. *J Neurosci*. 2009; 29:14394–14407. [PubMed: 19923274]
  78. Graff J, Mansuy IM. Epigenetic dysregulation in cognitive disorders. *Eur J Neurosci*. 2009; 30:1–8. [PubMed: 19508697]
  79. McShea A, Wahl AF, Smith MA. Re-entry into the cell cycle: a mechanism for neurodegeneration in Alzheimer disease. *Med Hypotheses*. 1999; 52:525–527. [PubMed: 10459833]
  80. Raina AK, Pardo P, Rottkamp CA, Zhu X, Pereira-Smith OM, Smith MA. Neurons in Alzheimer disease emerge from senescence. *Mech Ageing Dev*. 2001; 123:3–9. [PubMed: 11640946]

81. Evans TA, Raina AK, Delacourte A, Aprelikova O, Lee H-G, Zhu X, Perry G, Smith MA. BRCA1 may modulate neuronal cell cycle re-entry in Alzheimer disease. *Int J Med Sci.* 2007; 4:140–145. [PubMed: 17505559]
82. Jelinic P, Pellegrino J, David G. A novel mammalian complex containing Sin3B mitigates histone acetylation and RNA polymerase II progression within transcribed loci. *Mol Cell Biol.* 2011; 31:54–62. [PubMed: 21041482]
83. Tominaga K, Leung JK, Rookard P, Echigo J, Smith JR, Pereira-Smith OM. MRGX is a novel transcriptional regulator that exhibits activation or repression of the B-myb promoter in a cell type-dependent manner. *J Biol Chem.* 2003; 278:49618–49624. [PubMed: 14506250]
84. Tyteca S, Vandromme M, Legube G, Chevillard-Briet M, Trouche D. Tip60 and p400 are both required for UV-induced apoptosis but play antagonistic roles in cell cycle progression. *EMBO J.* 2006; 25:1680–1689. [PubMed: 16601686]
85. Gevry N, Chan HM, Laflamme L, Livingston DM, Gaudreau L. p21 transcription is regulated by differential localization of histone H2A.Z. *Genes Dev.* 2007; 21:1869–1881. [PubMed: 17671089]
86. Park JH, Sun XJ, Roeder RG. The SANT domain of p400 ATPase represses acetyltransferase activity and coactivator function of TIP60 in basal p21 gene expression. *Mol Cell Biol.* 2010; 30:2750–2761. [PubMed: 20351180]

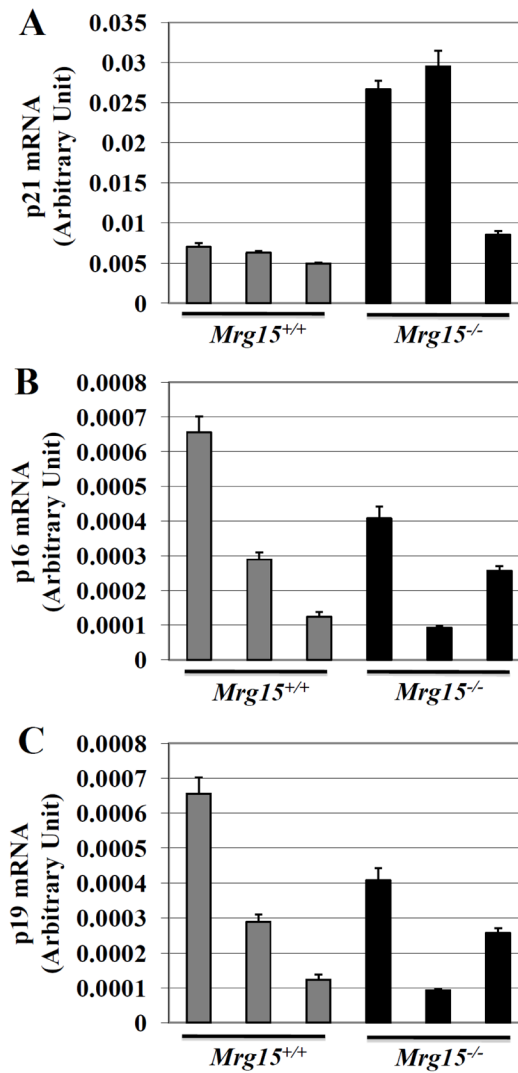


**Figure 1. Increased expression of p21, but not p16/p19 expression, in early passage E10.5 *Mrg15* deficient NSC cultures**

mRNA expression levels of p21 (A), p16INK4a (B), and 19ARF (C) genes was measured by qRT-PCR from three wild-type and three *Mrg15* deficient NSC cultures. Data was normalized to expression levels of the  $\beta$ -actin gene. Each data represents the average of three independent assays (mean  $\pm$  SEM).

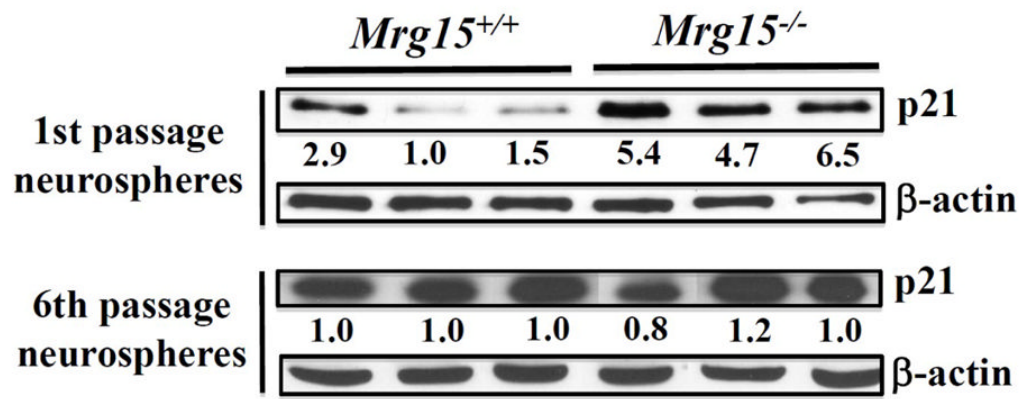


**Figure 2. p21 protein accumulation in NSC cultures**

A representative Western blot of p21 is shown. Total cell lysates were prepared from first or sixth passage of neurospheres from three wild-type and three *Mrg15* deficient embryos. Equal amounts of protein was loaded, transferred to nitrocellulose membrane, and probed with antibodies for p21 and β-actin (loading control).

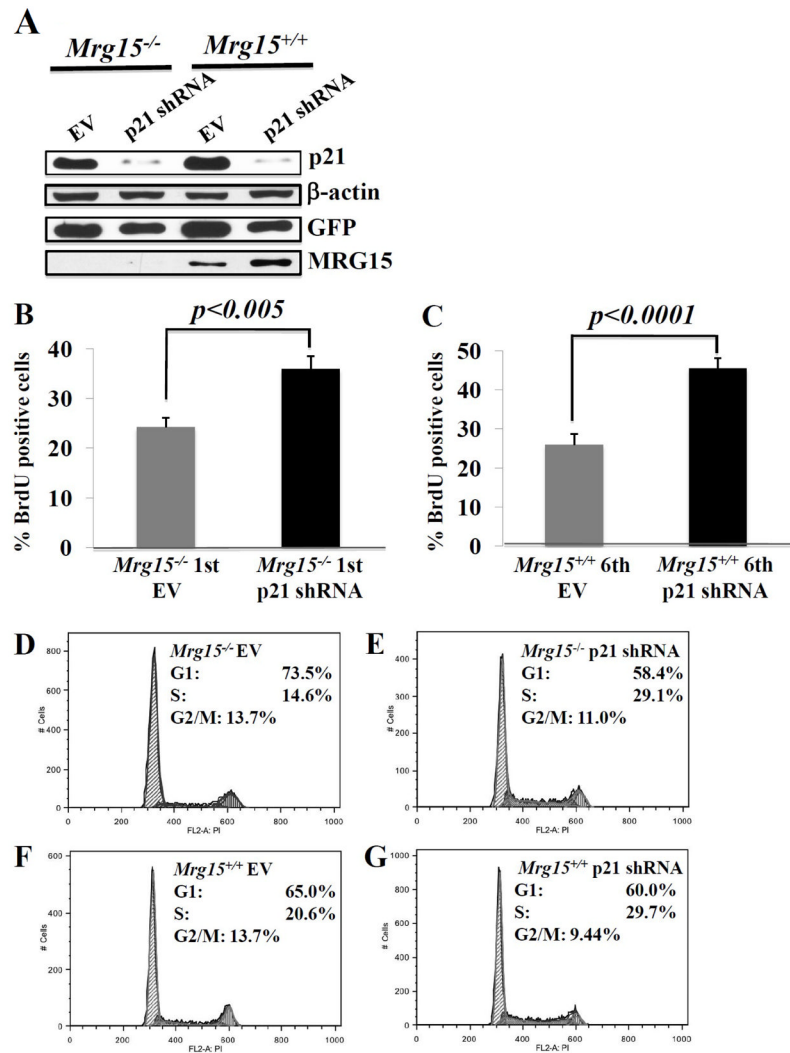


**Figure 3. p21 shRNA rescues cell proliferation in early passage (1st) *Mrg15* deficient NSCs and late passage (6th) wild-type NSCs**

(A) Cells expressing empty vector (EV) or p21 shRNA were analyzed by Western blot to p21,  $\beta$ -actin (loading control), GFP (indication of infection efficiency), and MRG15. (B, C) Representative BrdU immunostaining in *Mrg15* deficient cells (B) at first passage and wild-type cells (C) at sixth passage. Single cells were plated on poly-L-lysine-coated coverslips, grown for 48 h, and incubated with 10  $\mu$ M BrdU for 1 h. Incorporated BrdU was detected by mouse anti-BrdU antibody followed by incubation with biotinylated anti-mouse IgG and positive cells identified by DAB staining. The percentage of positive cells was determined by counting under a light microscope. Error bars represent standard error of mean (SEM) of triplicate counts and P values determined using unpaired t test. (D, E, F, G) Cell cycle distribution of GFP-positive *Mrg15* deficient and wild-type NSCs after infection with a GFP-expressing lentivirus containing empty vector or a p21 shRNA construct. (D) *Mrg15* deficient NSCs with empty vector. (E) *Mrg15* deficient NSCs with p21 shRNA construct. (F) wild-type NSCs with empty vector. (G) wild-type NSCs with p21 shRNA construct.



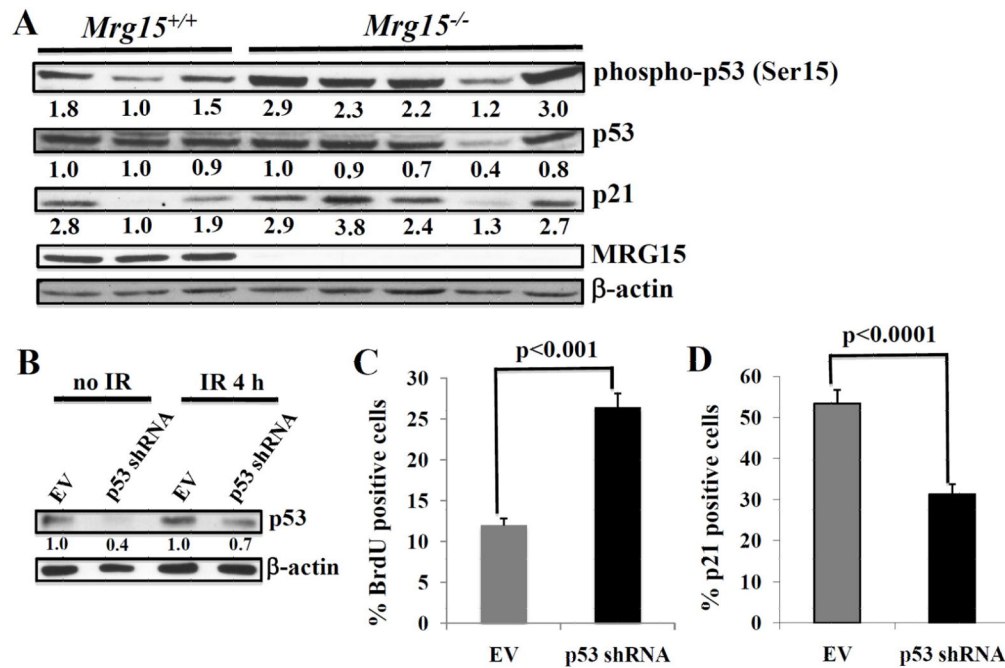


**Figure 4. Accumulation of activated p53 in *Mrg15* deficient NSC cultures and effects of p53 shRNA knockdown**

(A) A representative Western blot analysis of phosphorylated p53 at Ser15 is shown. Total cell lysates were prepared from early passage neurospheres from three wild-type and five *Mrg15* deficient embryos. Equal amounts of protein was loaded, transferred to nitrocellulose membrane, and probed with antibodies for phospho-p53 (Ser15), p53, p21, MRG15, and  $\beta$ -actin (loading control). (B) *Mrg15* deficient NSCs expressing empty vector (EV) or p53 shRNA were analyzed by Western blot to p53 and  $\beta$ -actin (loading control). (C) Percentage of BrdU positive cells in early passage of *Mrg15* deficient NSCs after lentivirus infection expressing EV or p53 shRNA. The percentage of BrdU positive cells by immunostaining was determined by counting under a light microscope. Error bars represent standard error of mean (SEM) of counts from ten fields and P values determined using unpaired t test. (D) Percentage of p21 positive cells in early passage of *Mrg15* deficient NSCs after lentivirus infection expressing EV or p53 shRNA. The percentage of p21 positive cells by immunostaining was determined by counting under a light microscope. Error bars represent standard error of mean (SEM) of counts from ten fields and P values determined using unpaired t test.

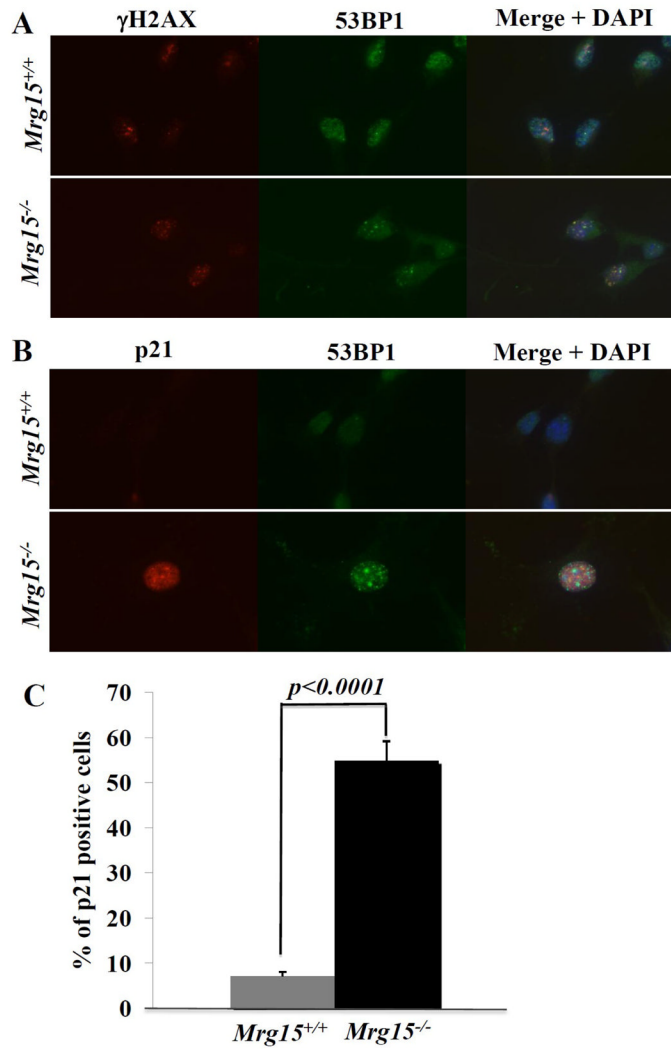


**Figure 5. Co-staining of p21 with DNA damage foci in *Mrg15* deficient NSCs**

(A) Detection of DNA damage foci in NSC cultures. Wild-type (upper panel) and *Mrg15* deficient (lower panel) NSCs were fixed and foci of  $\gamma$ H2AX (red) and 53BP1 (green) in nuclei detected by immunostaining. Nuclei were counterstained with DAPI. (B) Wild-type (upper panel) and *Mrg15* deficient (lower panel) NSCs were fixed, co-stained with mouse anti-p21 (red) and rabbit anti-53BP1 (green) antibodies, and counterstained with DAPI. Examples of p21/53BP1 foci double positive cells in merged images are shown in separate pictures. (C) Percentage of p21 positive cells in early passage NSC cultures. Error bars represent standard error of mean (SEM) from 8 field counts for wild-type and 12 field counts for *Mrg15* deficient cells. p values were determined using the unpaired t test. Representative data from two experiments is shown.

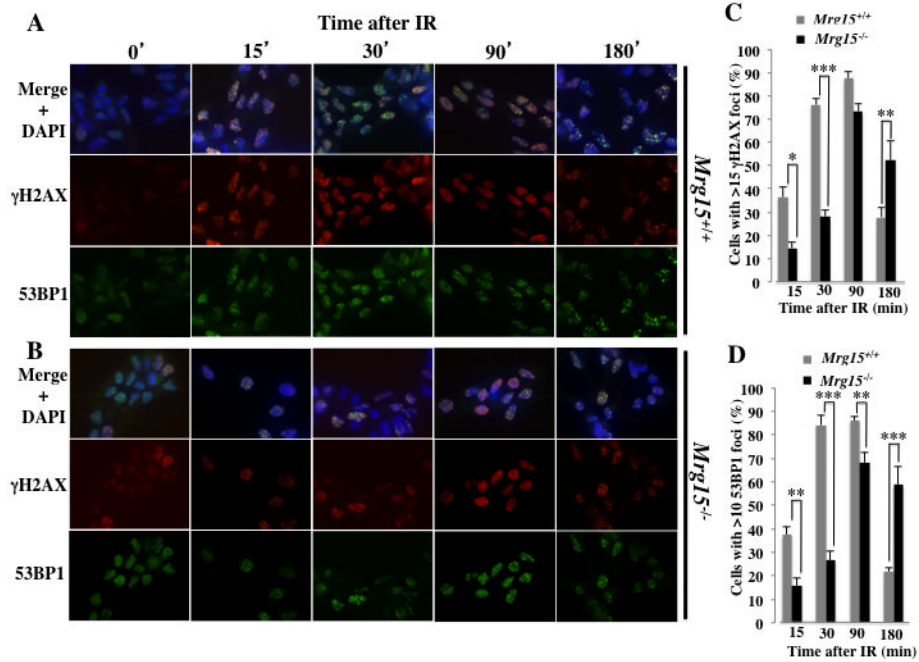


**Figure 6. Defects in DNA damage response in *Mrg15* deficient NSCs**

Wild-type (A) and *Mrg15* deficient (B) NSCs were fixed at 0, 15, 30, 90, and 180 minutes post exposure to 10 Gy, co-stained with mouse anti- $\gamma$ H2AX (red) and rabbit anti-53BP1 (green) antibodies, and counterstained with DAPI to visualize nuclei. Examples of co-localization of  $\gamma$ H2AX and 53BP1 foci in merged images are shown with separated pictures. Representative cells from two experiments are shown. (C) Quantification of cells with  $\gamma$ H2AX foci at 15, 30, 90, and 180 min after IR (mean  $\pm$  SEM, n=5). (D) Quantification of cells with 53BP1 foci at 15, 30, 90, and 180 min after IR (mean  $\pm$  SEM, n=5). p values determined using one-way ANOVA. Asterisk indicates,  $p < 0.05$ ; double asterisk indicates,  $p < 0.01$ ; triple asterisk indicates,  $p < 0.001$ .

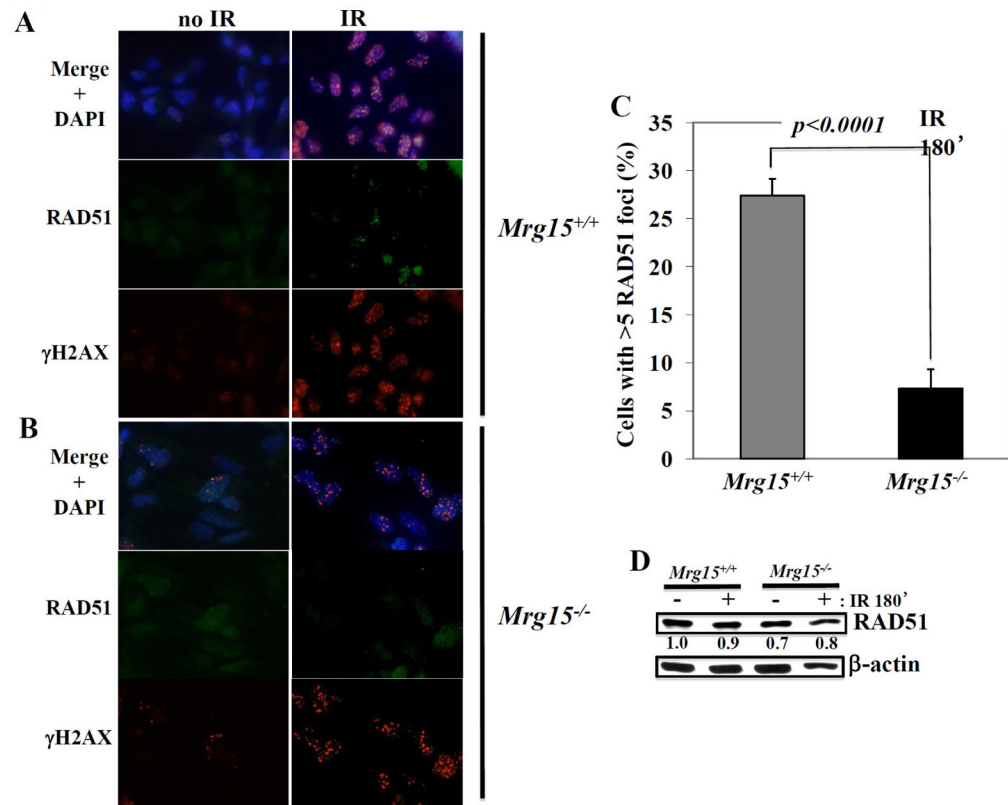


**Figure 7. Defects of RAD51 focus formation in *Mrg15* deficient NSCs after IR exposure**  
 Wild-type (A) and *Mrg15* deficient (B) NSCs were fixed with or without IR at 180 min post exposure, co-stained with rabbit anti-RAD51 (green) and mouse anti- $\gamma$ H2AX (red) antibodies, and counterstained with DAPI to visualize nuclei. Representative pictures for colocalization of RAD51 and  $\gamma$ H2AX in merged images are shown with separated pictures. Representative cells from two experiments are shown. (C) Quantification of cells with the RAD51 foci at 180 minutes after IR (mean  $\pm$  SEM, n=5). P values determined using unpaired t test. (D) Detection of RAD51 expression level by Western blot. Total cell lysates were prepared from NSCs with or without IR at 180 min post exposure and levels of RAD51 and  $\beta$ -actin (loading control) were detected by Western blot.